Single-phase Chromatography: Solute Retardation by Ultrafiltration and Electrophoresis

It is suggested that chromatographic separations can be performed very effectively in the absence of a stationary sorbent phase by using small diameter tubes or tube bundles for the column and segregating the solutes radially into the slower moving fluid near the tube walls. Separation is achieved by differential solute retardation whenever the degree of segregation is different for the various solute species present.

An approximate analysis and preliminary experimental studies demonstrate the feasibility of using ultrafiltration through the tube wall to achieve solute separation. Preliminary estimates based on our ultrafiltration analysis also show that segregation by electromigration is very promising for electrically charged solutes.

H.-L. LEE
J. F. G. REIS
JOHN DOHNER
and
E. N. LIGHTFOOT

Department of Chemical Engineering
University of Wisconsin
Madison, Wisconsin 53706

SCOPE

Two processes are described here for carrying out chromatographic separations without the stationary sorbent phase of conventional systems. Preliminary calculations and experiments demonstrate the feasibility of the proposed processes and suggest some substantial advantages over presently available possibilities. It is of particular interest that separations depend primarily upon differences in such transport properties as diffusivity and electrophoretic mobility: these separations are dominated by transport rather than equilibrium considerations.

CONCLUSIONS AND SIGNIFICANCE

The bulk of this paper deals with retardation by ultrafiltration, and the approximate analysis presented appears sufficient for preliminary assessment of this process.

On that basis it would appear that the ultrafiltration-based process is quite promising for small-scale fractionation of polymers, for example, in the determination of molecular-weight distributions. Here the potential sharpness of the separation, the predictability of retardation factors in terms of molecular structure, plus the general applicability and simplicity of the method can be put to good advantage. In large-scale separations the unavoidable loss of solvent through the tube walls, which tends to require large-diameter tubes, may present a problem. Further developmental work is needed here.

Only a very primitive analysis is presented for retardation by electrophoretic migration, but this permits useful predictions of separation potential if one notes its basic similarity to the ultrafiltration-based process and considers the related work of Caldwell et al. (1972) for slit-flow geometries.

Indications are that this process is quite promising over a very wide range of process requirements, from microanalysis in single tubes to industrial-scale separations. It is particularly noteworthy that three of the most severe problems of electrophoresis, excessive heating, convective-dispersion, and hydrodynamic instabilities can be simply controlled using the tubular geometry.

The purpose of the first part of this paper is to explore the possibilities of the ultrafiltration-induced single-phase chromatographic process illustrated in Figure 1. The second part consists of extending this to another process where a lateral electric field across the tube replaces the lateral solvent flux. We begin with a brief description of system operation immediately below and then proceed to develop a mathematical analysis suitable for our purposes. We conclude the first part with a summary of preliminary experiments, showing the feasibility of the proposed operation with presently available technology and a brief discussion of their significance.

RETARDATION BY ULTRAFILTRATION

As in more conventional types of chromatography, separation of two or more solutes is achieved by selectively retarding them relative to the solvent flowing through the column. In our operation this is achieved by using bundles of hollow fibers in lieu of a packed bed and segregating the solutes into the slow-moving fluid near the fiber walls rather than by distribution into a second, stationary, phase. Segregation in turn can be accomplished by either ultrafiltration of solvent through the fiber wall, which is the process considered here, or by electrophoretic migration in a superimposed electric field, which will be described below (part B). A nonuniform concentration profile will be established over the flow cross section, as indicated in Figure 1b, and its shape will depend upon the relative importance of the segregating effect, here radial convection, and the back diffusion of the segregated solutes. For our situation, degree of segregation, and hence solute retardation, will be governed by the Péclet number

$$Pé \equiv v_w R/\mathcal{D}_{im} \quad (1)$$

where v_w is radial solute velocity at the wall, R is tube radius, and $\mathcal{D}_{im}$ is the effective binary diffusivity of a given solute species i. As one would expect, retardation becomes more effective for larger $Pé$; it is already significant for $Pé = 1$.

As in more conventional procedures the only essential steps in our process are charging a relatively small volume of the solution to be processed into the upstream end of the column and then successively eluting the individual solutes by continuing addition of solvent. This differs from normal chromatographic operations only in that ultrafiltration is maintained at all times by keeping the intrafiber space at elevated pressure.

However, we find that much improved separations may be obtained if the feed solution is held at the upstream end of the column long enough to allow radial redistribution of solutes before the start of elution. This is because radial migration is slow and because feed concentration is initially very nearly uniform over fiber cross sections. We have also found that solute can be focused into a very small length of fiber during this initial holding period by feeding solvent into both ends of the column. The axial position of the resulting solute bolus can be controlled very simply and effectively by adjusting the relative flow rates to the two ends of the column.

It appears from our preliminary experiments, described later in this paper, that this simple technique is very effective for a wide variety of solutes, particularly high polymers, and that it can be adapted to a very wide range of flow rates. We discuss these points further after a mathematical analysis and presentation of data.

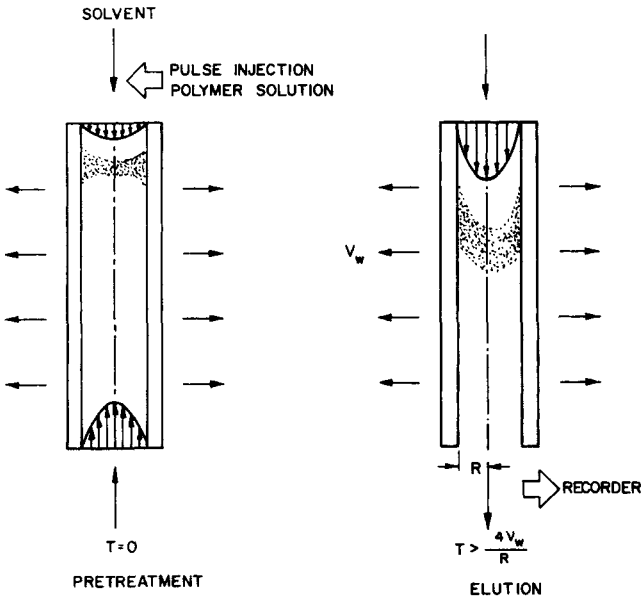

Fig. 1a. Operation of single-phase chromatograpry using hollow fibers.

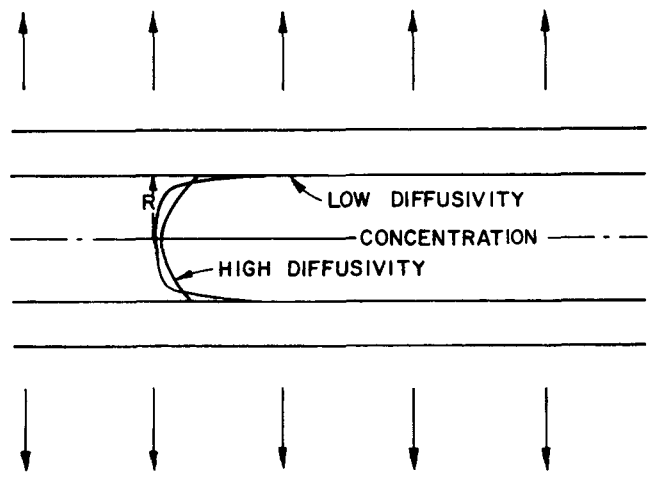

Fig. 1b. Typical concentration profiles needed for single-phase chromatography.

EXPECTATION

Here we develop a description of the above-described chromatographic process which appears to be adequate for assessing its potential and for planning a systematic experimental investigation. The key elements of this description are equations for predicting the average axial velocity of solutes down the column relative to the solvent, the time required for initial radial distribution of solutes at the column inlet, and the convective dispersion of solute during elution. We begin by defining our system and proceed by a method analogous to that used by Gill and Sankarasubramanian (1970) to describe Taylor dispersion.

System Definition

We begin by considering a single tube and by assuming negligible osmotic effects and that pressure drop along the tube axis is small compared to that across the tube wall. We also note that for presently available fibers

$$\frac{\partial \ln \langle v_z \rangle}{\partial (z/R)} << 1 \quad (2)$$

where $\langle v_z \rangle$ is flow-average axial velocity and z is distance along fiber axis. System hydrodynamics is then adequately described (see, for example, Kozinski et al., 1970) by

$$v_z = 2\langle v_z \rangle [1 - (r/R)^2] \quad (3)$$

$$v_r = v_w [2(r/R) - (r/R)^3] \quad (4)$$

$$\frac{\partial \langle v_z \rangle}{\partial z} = -2v_w/R \quad (5)$$

where v_w is the radial velocity at the fiber wall, independent of z for our assumptions, and r is radial distance from the fiber axis.

Mass transfer is adequately described by the axially symmetric continuity relation for species i, i being a solute,

$$\frac{\partial c_i}{\partial t} + \frac{1}{r}\frac{\partial}{\partial r} r N_{ir} + \frac{\partial N_{iz}}{\partial z} = 0 \quad (6)$$

and the pseudobinary form of Fick's law*:

$$N_{ir} = -\mathcal{D}_{im}\frac{\partial c_i}{\partial r} + v_r c_i \quad (7a)$$

$$N_{iz} = -\mathcal{D}_{im}\frac{\partial c_i}{\partial z} + v_z c_i \quad (7b)$$

Here c_i is molar concentration of species i, $\underline{N}_i = c_i \underline{v}_i$ is the molar flux of species i, and $\mathcal{D}_{im}$ is its effective binary diffusivity through the mixture m; $\mathcal{D}_{im}$ will be considered to be constant.

Boundary conditions on radial transport are that

$$N_{ir} = 0 \quad \text{at} \quad r = 0, R \quad (8, 9)$$

* Note that we are dealing with a multicomponent mixture. For a discussion of $\mathcal{D}_{im}$, see Lightfoot (1974).

and boundary conditions on axial transport will be given later.

To obtain a description of the chromatographic operation we put Equations (7) into (6) and average over the flow cross section using Equations (8) and (9). This gives

$$\frac{\partial \langle c_i \rangle}{\partial t} + \frac{\partial}{\partial z}\langle v_z c_i \rangle - \mathcal{D}_{im}\frac{\partial^2 \langle c_i \rangle}{\partial z^2} = 0 \qquad (10)$$

which eliminates radial dependence. Here

$$\langle Q \rangle = \int_0^R Q r dr \Big/ \int_0^R r dr \qquad (11)$$

where Q is any quantity. We next postulate a series solution of the form

$$c_i = \sum_{k=0}^{\infty} f_k(r,t)\frac{\partial^k \langle c_i \rangle}{\partial z^k}\langle v_z \rangle^k \qquad (12)$$

Note that the zeroth derivative in this expression is just $\langle c_i \rangle$. Equation (12) then permits us to rewrite Equation (10) in the form

$$\frac{\partial \langle c_i \rangle}{\partial t} + \sum_{k=0}^{\infty}\frac{\partial}{\partial z}\left(\langle v_z \rangle^k \langle v_z f_k \rangle \frac{\partial^k \langle c_i \rangle}{\partial z^k}\right) - \mathcal{D}_{im}\frac{\partial^2 \langle c_i \rangle}{\partial z^2} = 0 \qquad (13)$$

We now note that Gill and Sankarasubramanian (1970) found all derivatives higher than the second in Equation (13) to be unimportant for Taylor dispersion ($v_r = 0$). We also neglect them here and thus obtain

$$\frac{\partial \langle c_i \rangle}{\partial t} + \frac{\partial}{\partial z}(\bar{u}\langle c_i \rangle) = \frac{\partial}{\partial z}\bar{D}\frac{\partial \langle c_i \rangle}{\partial z} \qquad (14)$$

with

$$\bar{u} = \langle v_z f_0 \rangle \qquad (15)$$

$$\bar{D} = \mathcal{D}_{im} - \langle v_z f_1 \rangle \langle v_z \rangle \qquad (16)$$

This is formally similar to the one-dimensional diffusion equation, but the effective convective velocity $\bar{u}$ and diffusivity $\bar{D}$ are dependent upon both axial position and time.

Equations (14) through (16) complete the mathematical definition of our model system, and it only remains to evaluate the parameters $\bar{u}$ and $\bar{D}$, and to integrate Equation (14) for appropriate initial and boundary conditions. We do this shortly, but first we define a retardation factor widely used by workers in chromatography as

$$R_f = \frac{\text{average velocity of solute}}{\text{average velocity of solvent}} \qquad (17a)$$

$$= \frac{\langle v_z c_i \rangle}{\langle v_z \rangle \langle c_i \rangle} \qquad (17b)$$

Equation (17b) may be written in the alternate form

$$R_f = \frac{\bar{u}}{\langle v_z \rangle} = \frac{\langle v_z f_0 \rangle}{\langle v_z \rangle} \qquad (18)$$

since $\langle f_0 \rangle$ is by definition unity. Equation (18) will be seen to give useful insight into the behavior of our system.

To determine f_0 and f_1, and hence the desired (approximate) description of our system we first assume that solute pulses are always sufficiently sharp so that

$$\left(\frac{\partial \ln c_i}{\partial \ln v_z}\right)_{r,t} >> 1 \qquad (19)$$

which permits us to neglect the fractional axial variation of v_z. This necessarily introduces error in f_0 and f_1, but should be a good approximation for situations of interest to us, especially for high polymers where desirable wall permeation velocities v_w are small relative to $\langle v_z \rangle$.

Combining Equation (12) with (6) and (7), using Equation (14) to eliminate the time derivatives of $\langle c_i \rangle$ and equating coefficients of $\langle c_i \rangle$ and $\partial \langle c_i \rangle / \partial z$, we obtain*

$$\frac{\partial f_0}{\partial t} + \frac{1}{r}\frac{\partial}{\partial r}\left[r\left(v_r f_0 - \mathcal{D}_{im}\frac{\partial f_0}{\partial r}\right)\right] = 0 \qquad (20)$$

with

$$v_r f_0 - \mathcal{D}_{im}\frac{\partial f_0}{\partial r} = 0 \quad \text{at} \quad r = 0, R \qquad (21)$$

$$\langle f_0 \rangle = 1 \qquad (22)$$

and

$$\frac{\partial f_1}{\partial t} + \frac{1}{r}\frac{\partial}{\partial r}\left[r\left(v_r f_1 - \mathcal{D}_{im}\frac{\partial f_1}{\partial r}\right)\right] + \frac{f_0(v_z - \langle v_z f_0 \rangle)}{\langle v_z \rangle} = 0 \qquad (23)$$

with

$$v_r f_1 - \mathcal{D}_{im}\frac{\partial f_1}{\partial r} = 0 \quad \text{at} \quad r = 0, R \qquad (24)$$

$$\langle f_1 \rangle = 0 \qquad (25)$$

Initial conditions are complex in our situation and not entirely unambiguous. We discuss these separately for the holding and elution periods below.

Description of Initial Solute Redistribution

We consider here a narrow band of solute held near the column inlet by solvent feed into both ends of the fibers. Our purpose is to determine the asymptotic radial concentration profile reached on prolonged holding and the time needed to approximate this asymptotic condition. During this period N_{iz} will be close to zero everywhere, and at its beginning radial solute distribution will be nearly uniform.

We are thus only interested in f_0, and we may choose as our initial condition

$$f_0(r, 0) = 1 \qquad (26)$$

This choice is consistent with Equation (22), and it is conservative since some solute redistribution will occur during establishment of the band in the column.

We next note that there is no need for highly accurate description of the transient period, and we therefore content ourselves with the approximation

$$f_0 = \frac{4e^{-4\tau}}{[2 - \eta^2(1 - e^{-4\tau})]^2} + \left(\frac{1 - e^{-4\tau}}{1 + e^{-4\tau}}\right)\frac{\exp\left[Pé\left(\eta^2 - \frac{1}{4}\eta^4\right)\right]}{\left\langle \exp\left[Pé\left(\eta^2 - \frac{1}{4}\eta^4\right)\right]\right\rangle} \qquad (27)$$

where $\eta = r/R$ and $\tau = tv_w/R$. Equation (27), in addition to being simple, is exact at all times in the limit of large $Pé$ and at large time for all $Pé$. It is quite adequate for our purposes, and it suggests that a holding period of the order of $\tau = 1$ is sufficient.

* Terms containing $\partial \langle v_z \rangle / \partial z$ neglected as a consequence of Equation (19).

Description of Elution

The transition from the holding period to the start of elution is characterized by an abrupt change in the axial velocity distribution. Providing that the hydrodynamic transients die out quickly, the radial flow pattern is not expected to be greatly disturbed. The radial distribution of solute can then be considered continuous across this period of transition, whereas such mathematical constructs as f_0 and f_1 etc. cannot. It is therefore simplest to describe the elution period apart from the holding period and to connect the two by assuming the continuity of concentration profiles. This approach leads to the initial conditions,

$$f_0 = \frac{e^{Pé\left(\eta^2 - \frac{1}{4}\eta^4\right)}}{\left\langle e^{Pé\left(\eta^2 - \frac{1}{4}\eta^4\right)} \right\rangle} \tag{28}$$

$$f_i = 0; \quad i \geq 1 \tag{29}$$

It is therefore unnecessary to resolve for the transient part of Equation (20): it is possible to use Equation (28) throughout the elution period. It follows that the retardation factor is constant and given by

$$R_f = \frac{\bar{u}}{\langle v_z \rangle} = \frac{4(e^{-Pé/4} - e^{-Pé})}{\sqrt{\pi Pé}\,(\operatorname{erf}\sqrt{Pé} - \operatorname{erf}\sqrt{Pé/4})} - 2 \tag{30}$$

obtained from Equations (18) and (28). For sufficiently high Péclet number Equation (30) reduces to

$$\lim_{Pé\to\infty} \{R_f\} = \frac{4}{Pé} \tag{31}$$

Equations (30) and (31) are compared graphically in Figure 2.

It is perhaps interesting to note that Equation (31) may also be obtained by a boundary-layer analysis in which all concentration changes of interest are assumed to take place near the fiber wall, $y = R - r << R$. For this situation v_r is just v_w and

$$f_0 = \frac{Pé}{2} e^{-yv_w/D_{im}} \tag{32}$$

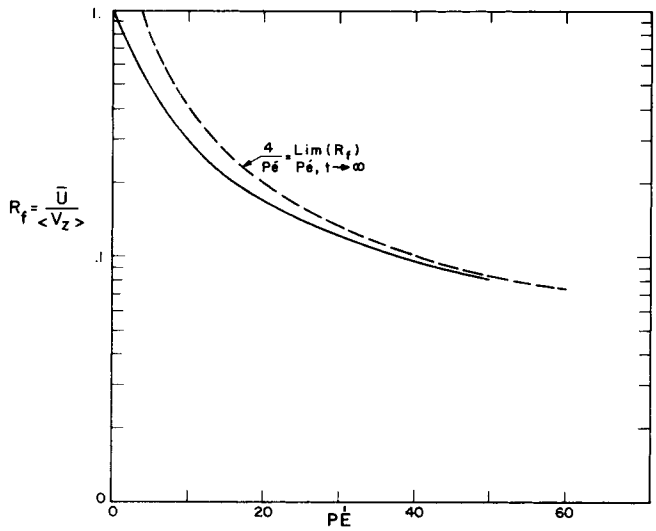

Fig. 2. Retardation factor as a function of Péclet number for chromatography in hollow-fiber ultrafilter.

Equation (32), plus the approximation for axial velocity

$$v_z = 4\langle v_z \rangle \frac{y}{R} \tag{33}$$

can be combined to give Equation (31).

Calculation of f_1, and hence $\bar{D}$, is unfortunately more complex. For our purpose no exact solution of Equation (23) is attempted. Rather we solve it exactly for the steady state limit $\bar{D}_\infty$ and account for the transient using the approximate expression

$$\bar{D} \doteq \bar{D}_\infty(1 - e^{-\lambda t}) \tag{34}$$

where λ^{-1} is some estimated response time of the system. From the previous discussion on holding period and the similarity between the equations involving the transient parts of functions f_0 and f_1

$$\lambda \doteq \frac{4v_w}{R} \quad \text{for large } Pé \tag{35}$$

We may now focus attention on the steady state part, $f_{1\infty}$. This asymptotic value, obtained by integrating Equation (23) with $\partial f_1/\partial t = 0$, is

$$f_{1\infty} = f_0 \int_0^\eta \frac{\int_0^{\eta'} (v_z - \bar{u})\, f_0 \eta'' d\eta''}{\langle v_z \rangle \eta' f_0} d\eta' + Kf_0 \tag{36}$$

where K is a constant determined from the condition $\langle f_1 \rangle = 0$. Then by suitable changes of the orders of integration

$$\bar{D}_\infty - \mathcal{D}_{im} = -\langle v_z \rangle \langle v_z f_{1\infty} \rangle = \frac{(R\langle v_z \rangle)^2}{\mathcal{D}_{im}} \int_0^1 \frac{\left[\int_0^{\eta'} \left(\frac{v_z}{\langle v_z \rangle} - R_f\right) f_0 \eta d\eta\right]^2}{\eta' f_0} d\eta' \tag{37}$$

We have calculated this integral numerically for $Pé$ up to 70 and plotted the results in Figure 3.

For very large Péclet number the boundary layer approximation can again be made. In this way one obtains

$$\lim_{Pé\to\infty} \{\bar{D}/\mathcal{D}_{im}\} = 1 + \frac{32}{Pé^4}\left(\frac{\langle v_z \rangle R}{\mathcal{D}_{im}}\right)^2 \tag{38}$$

$$= 1 + \frac{32}{Pé^2}\left(\frac{\langle v_z \rangle}{v_w}\right)^2 \tag{39}$$

which is reminiscent of Taylor dispersion. This result, also plotted in Figure 3, appears to be reasonably accurate for $Pé > 10^2$; it overestimates dispersion at lower $Pé$.

It may next be noted that even if all entering fluid leaves through the fiber walls

$$\frac{\langle v_z \rangle_{avg}}{v_w} = (L/R) \tag{40}$$

which is always much larger than unity. It can be shown from Equations (39) and (40) that convection-induced dispersion is thus much more important than axial diffusion except at very high Péclet numbers; the latter will therefore be neglected here.

Calculation of Effluent Curves

We are now in a position to integrate Equation (14) for any initial conditions and Péclet number, but we must remember that

$$\langle v_z \rangle = \langle v_{z0} \rangle - \frac{2v_w z}{R} \tag{41}$$

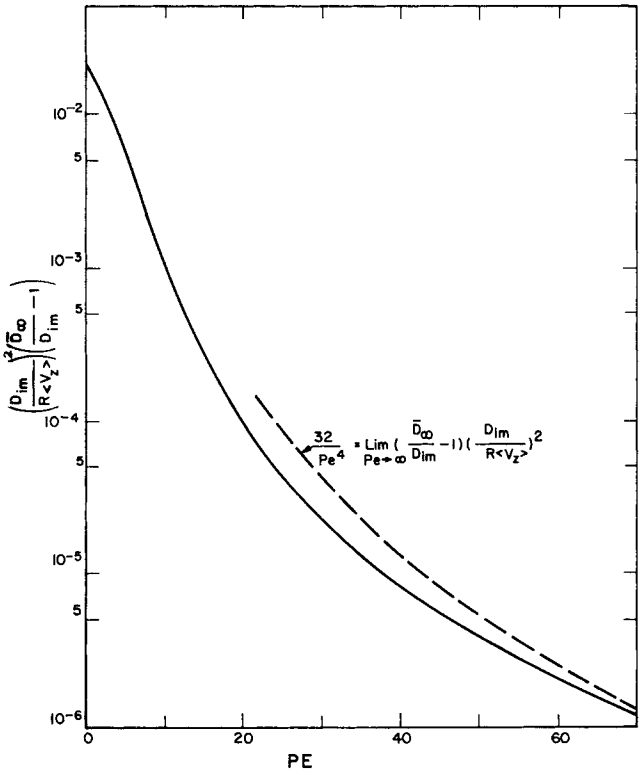

Fig. 3. Axial convective dispersion in fiber as a function of Péclet number.

where $\langle v_{z0} \rangle$ is the flow-average axial velocity at the inlet. It follows from Equation (30) that $\bar{u}$ is a function of z and from Equations (34) and (37) that $\bar{D}$ is a function of both z and t.

It is thus convenient to rewrite Equation (14) using the modified variables:

$$\theta = \frac{1}{L^2} \int_0^t \bar{D}(0,t)\,dt \tag{42}$$

$$\zeta = \frac{\Lambda}{L} \ln\left(\frac{1}{1 - z/\Lambda}\right) - \frac{\bar{u}(0)}{L} t - \frac{L}{\Lambda}\theta \tag{43}$$

where

$$\Lambda = \frac{R\langle v_{z0} \rangle}{2v_w} \tag{44}$$

is the length of column just sufficient to ultrafilter all incoming solvent, and

$$S = \langle c_i \rangle\, e^{-\frac{\bar{u}(0)}{\Lambda} t} \tag{45}$$

We thus obtain

$$\frac{\partial S}{\partial \theta} = \frac{\partial^2 S}{\partial \zeta^2} \tag{46}$$

in place of Equation (14). Equation (46) is just the one-dimensional form of Fick's second law, for which solutions are readily available. It is, however, not always easy to write initial conditions in terms of ζ.

We consider here as an illustrative example introduction of a short solute pulse to the column, with elution following a holding period as described above. We neglect entrance and exit effects and use the boundary condition

$$\int_{-\infty}^{\Lambda} \langle c_i \rangle \frac{dz}{L} = M_i \tag{47}$$

Integration of Equation (46) for this situation gives

$$\langle c_i \rangle = \frac{M_i}{2\sqrt{\pi\theta}}\, e^{-\zeta^2/4\theta + \frac{\bar{u}(0)}{\Lambda} t} \tag{48}$$

Note that $\Lambda/\bar{u}(0)$ is proportional to the radial response time R/v_w.

In order to show that a complete separation can occur, Equation (48) was used to construct the effluent curves of Figure 4 for assumed conditions which are roughly consistent with those for our experimental operations described below. Due to the approximations made in the analysis, no comparison of theory with experiment is attempted at this stage. Good separation is predicted for solutes whose diffusivities differ by more than a factor of 2 for *Pé* greater than 10. Better separations can be obtained in longer columns, but it must be remembered that there is a maximum length Λ for each flow rate. Optimization is therefore complicated by such physical constraints on the system variables.

OBSERVATION

We present here the results of preliminary experiments performed to determine the salient characteristics of ultrafiltration-induced single-phase chromatography. These experiments are qualitative in nature, in part because truly suitable apparatus is not yet available, and they should be extended. Even these preliminary results, however, show promise for effective separations.

Apparatus

The experimental set-up, shown in Figure 5, is based upon a Bio-rad 80 ultrafilter which has approximately the following characteristics:

Tube internal diameter: 2×10^{-2} cm
Ultrafiltration surface: 10^3cm^2
Total flow cross section: 0.4 cm^2
Total internal volume: 7 ml
Active volume: 5 ml (volume in which ultrafiltration can occur)
Nominal molecular-weight cut-off: 30,000
Nominal maximum ultrafiltration pressure: 83 kN/m^2 (12 lb./sq.in.)
Water permeability: 2/3 ml/min., lb./sq.in.

This unit was used for its high water permeability and because

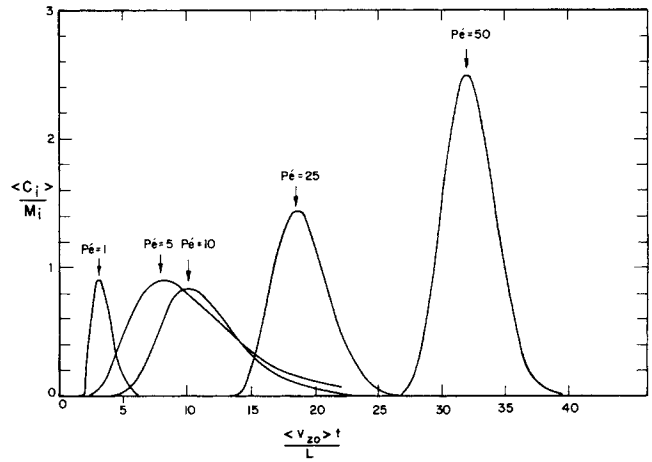

Fig. 4. Concentration measured at a distance 0.9 Λ from initial location of solute band as a function of time and Péclet number. The band width is 0.09 Λ initially. The significance of Λ is indicated in Equation (44).

it proved capable of withstanding much higher than rated pressure: experiments were made successfully at pressures as high as 275 kN/m² (40 lb./sq.in.).

Typical wall permeation velocities were about 3×10^{-4} cm/s so that Péclet numbers greater than unity can be obtained for solute diffusivities

$$\mathcal{D}_{im} = Rv_w/Pé \leq (10^{-2}\,\text{cm})(3 \times 10^{-4}\,\text{cm/s})/(1)$$
$$= 3 \times 10^{-6}\,\text{cm}^2/\text{s}$$

The experimental conditions obtainable in this apparatus are therefore just sufficient to obtain significant retardation of typical globular proteins.

The remainder of the equipment consisted primarily of rotameters for metering the flow, valves to control pressure and flows to the two ends of the column, and a Gilford spectrophotometer equipped with a flow cell of 0.3 ml volume.

Procedures

Two types of experiments were performed. In the first, valve B (see Figure 5) was closed, and solvent, essentially water, was pumped at a constant flow rate through the ultrafilter. Small pulses of solute (0.5 to 1.0 ml) were added through the injection port from a syringe, and the outlet concentration was monitored continuously.

In the second set, flow was initially maintained into both ends of the ultrafilter with the result that solute pulses became positioned at the point of no axial flow. In the case of blue dextran the solute was visible as a small blue spot in each tube, and it normally appeared very close to the expected position. This situation was maintained long enough for the solute to obtain a steady radial concentration distribution, normally about two min. This is of the order of (R/v_w), the radial distributions time constant of the previous section. After this initial holding period valve B was closed, and solute was eluted just as in the first type of experiment.

Solutes used included 0.2% blue dextran (from Pharmacia Corporation), human plasma diluted 1 to 5 (produced by centrifuging whole blood), and $CuSO_4$, which was used as a marker since it moved with the water through the tube walls. All three solutes were monitored at 262.5 mμ.

RESULTS

A typical concentration history for the first type of experiment (no pretreatment) is shown in Figure 6. Here 0.5 ml pulses of 0.2% blue dextran and 10% $CuSO_4$ were separately injected and the outlet concentration curves superimposed. It can be seen that the great bulk of blue dextran was significantly retarded, in accordance with expectation, but that a small amount moved with essentially the speed of the $CuSO_4$. This is apparently material initially near the center of the tube and which did not have time to migrate to the walls.

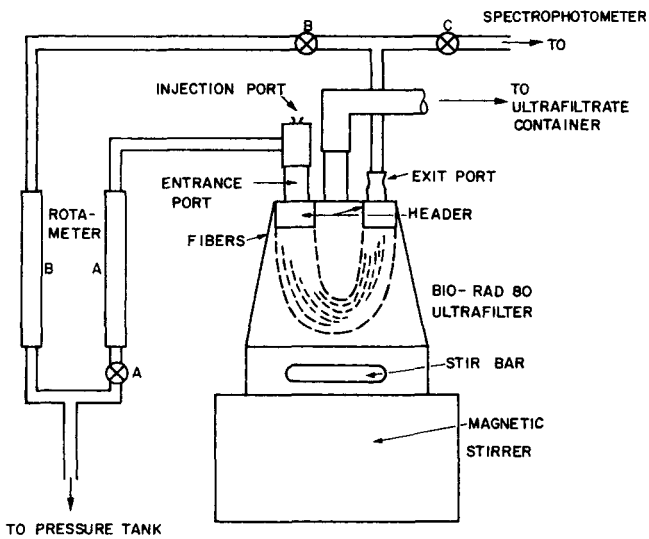

Fig. 5. Experimental apparatus used to demonstrate solute's retardation by ultrafiltration.

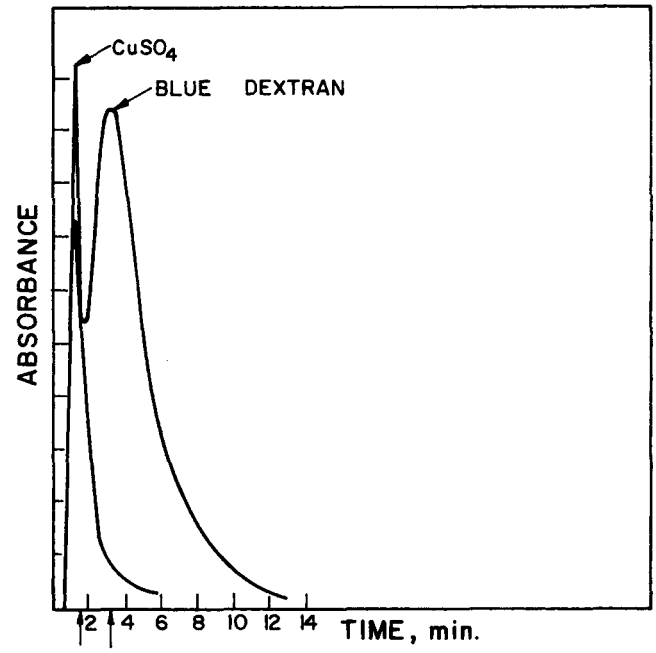

Fig. 6. Superimposed copper sulfate and blue dextran peaks obtained without pretreatments. The pressure difference across fiber's wall was 72 kN/m². Wall permeation rate was 17.7 ml/min. Eluent was collected at 2.5 ml/min. 0.5 ml of 0.2% blue dextran solution was injected for one curve and 0.5 ml of 10% copper sulfate for the other.

The effect of pretreatment is shown in Figure 7 where curves for blue dextran with and without pretreatment are superimposed. It can be seen that pretreatment eliminates the secondary peak and also appears to increase retardation of the main peak.

Figure 8 shows exit concentration as a function of time for chromatography of blood plasma, with pretreatment. The pressure, though a moderate 377 kN/m² (40 lb./sq.in.gauge), is the largest that can be obtained with our experimental set up without leakage and flow disturbances. The small multiple peaks near the maximum suggest partial fractionation of the plasma, but it is clear that the present equipment is not satisfactory for this purpose. It appears further experiments have to be done with longer fibers and higher pressures to effect a significant separation.

DISCUSSION

The expectation that significant solute separations can be obtained by ultrafiltration-based single-phase chromatography is borne out by our preliminary observations. Since this process appears economical and unlikely to damage even sensitive materials such as native proteins, it is deserving of further development.

The next step should be to fabricate fiber bundles which are longer and operable at higher pressures, preferably up to the bursting strength of the fibers. It is also desirable to explore the use of larger fibers, since

$$-\frac{1}{\langle v_{z0}\rangle}\frac{d\langle v_z\rangle}{dz/L} = 2Pé\frac{\mathcal{D}_{im}L}{\langle v_{z0}\rangle R^2}$$

Thus the fractional drop in axial velocity with distance into the column drops with the square of tube radius if the Péclet number, hence R_f, is maintained constant. It may be noted that the Péclet number at bursting pressure

is insensitive to tube radius if geometric similarity and constant mechanical properties can be maintained.

The decrease in axial velocity is an apparent drawback to this technique in that it limits column length for a given input flow rate. However, the radial segregation produced by the ultrafiltration also reduces axial dispersion. Considerable experiment and analysis will probably be required to evaluate this process, which presents a number of novel features. It may be noted here that electrophoretic segregation described below eliminates the loss of solvent through the tube wall.

RETARDATION BY A TRANSVERSE ELECTRICAL FIELD

The above-described limitation on column length can be avoided by use of other segregating techniques. For charged solutes perhaps the most convenient of these is a transverse electrical field, as pictured in Figure 9. Such an approach has already been shown by Caldwell et al. (1972) to be effective for slit flow, and the preliminary analysis we present here suggests it to be quite promising for the far more practical tubular geometry of most interest to us. To show this we first calculate retardation factors for the idealized but representative situation of Figure 9 and then examine the effect of tube walls on the interior potential distribution.

We assume continued steady feed of any solution to the top of the column and a uniform transverse electrical field; solute concentration is then independent of axial position, and if the electric field

$$\underline{E} = \underline{\delta}_x E = \text{const.} \tag{49}$$

the electrophoretic velocity of any species i will be

$$\underline{\epsilon}_i = \underline{\delta}_x u_i E \tag{50}$$

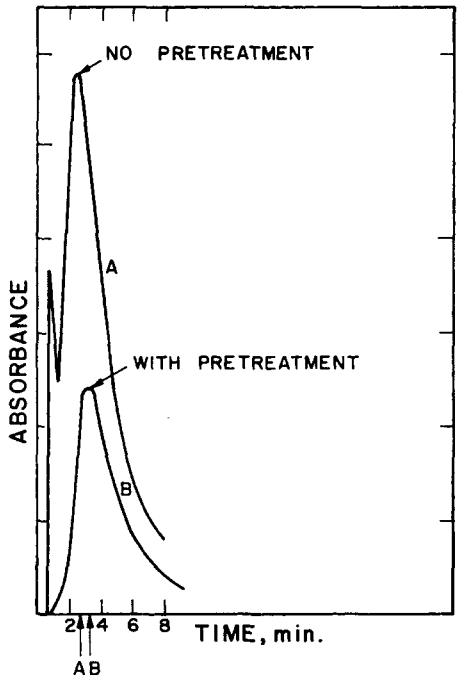

Fig. 7. Effect of pretreatment on output blue dextran peak. Curve A, was obtained without pretreatment and curve B for 2 min. initial holding. A smaller amount of dextran was used for curve B. In both cases the pressure used was 30 lb./sq.in. gauge. Permeation rate obtained was 19.6 ml/min. Eluents were collected at 2.2 ml/min.

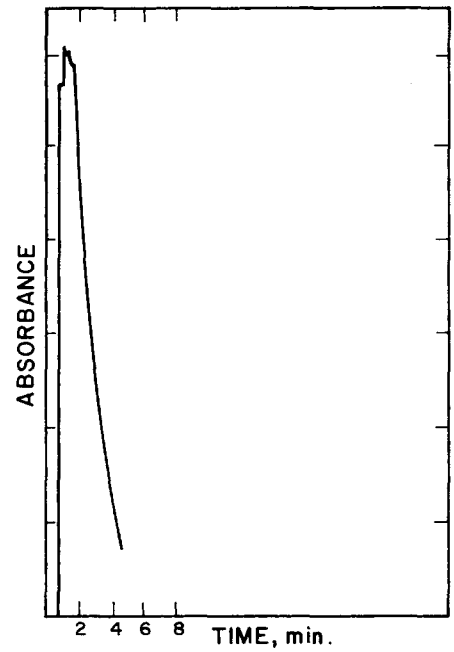

Fig. 8. Peak obtained with 0.5 ml of 20% plasma solution injected. Pressure difference across fiber's wall was 275 kN/m² (40 lb./sq.in.). Permeation rate was 22.5 ml/min. Eluent was collected at 1.4 ml/min.

where u_i is the electrical mobility. The defining equation for the solute distribution is then, if the solution is dilute:

$$\epsilon_i c_i - \mathcal{D}_{im} \frac{\partial c_i}{\partial x} = 0 \tag{51}$$

where $\mathcal{D}_{im}$ is the effective binary diffusivity of i through the mixture m. Then

$$\frac{c_i}{c_{i0}} = e^{x\epsilon_i/D_{im}} = e^{\eta\cos\phi(\epsilon_i R/D_{im})} \tag{52}$$

Here c_{i0} is solute concentration at the tube axis, r and ϕ are cylindrical coordinates as indicated, and $\eta = r/R$, where R is tube radius. The ratio $\epsilon_i R/\mathcal{D}_{im}$ is a Péclet number for the process and will be designated by $Pé$.

The solvent velocity profile may normally be considered to be parabolic

$$v_z = v_{\max}(1 - \eta^2) \tag{53}$$

and therefore

$$R_i = 2\left\{1 - \frac{\int_0^\pi \int_0^1 e^{\eta\cos\phi Pé}\eta^3 d\eta d\phi}{\int_0^\pi \int_0^1 e^{\eta\cos\phi Pé}\eta d\eta d\phi}\right\} \tag{54}$$

We have not found a compact representation of this expression, but we can express it in the series form

$$R_i = 1 - \frac{\sum_{k=1}^{\infty} \frac{Pé^{2k}}{M_k}}{\frac{1}{2} + \sum_{k=1}^{\infty} \frac{(k+2)Pé^{2k}}{kM_k}} \tag{55a}$$

where

$$M_k = k^{2k+1}(k-1)!(k+2)! \tag{55b}$$

This expression is readily evaluated numerically, and representative results are shown in Figure 10.

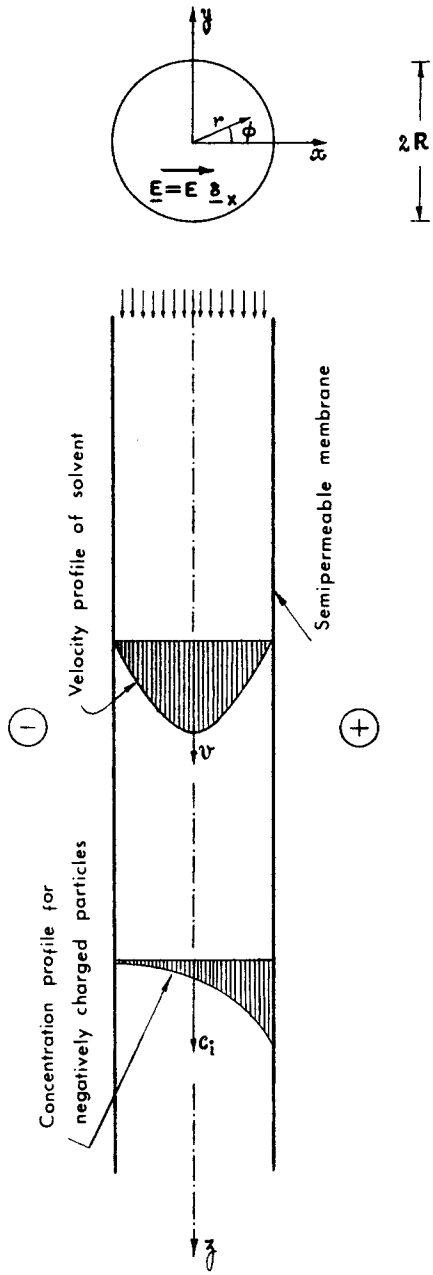

Fig. 9. Schematic representation of the system treated. Solution is fed to the fiber in steady laminar flow. The fiber wall is assumed to have an ionic conductance comparable to that of the feed solution and surrounding electrolyte. Note that in an actual chromatographic separation a short pulse of mixed solute would be injected initially and followed by feed of pure solvent.

It is shown here that very significant retardations are readily achieved for relatively low potential gradients. It should be noted in this respect that gradients of from 6 to 50 V/cm have been used routinely in systems of similar configuration. The tube radii and mobilities used in the calculations are representative of commercially available ultrafiltration fibers and common globular proteins.

The system shown is batch in nature and eminently suitable for the small-scale separations characteristic of electrophoresis today. As an example analytic separations can be carried out with single fibers. However, it should also be possible to scale up almost indefinitely by use of large fiber bundles. The small diameter of typical fibers and the segregation of solute into thin boundary layers also tend to stabilize the system against free convection and thus eliminate the need for a packing. Also the loose nature of a fiber bundle combined with the small fiber radii permits very effective convective cooling. Our proposed system thus appears to offer significant practical advantage over more conventional devices.

The success of this approach does of course depend upon achieving an adequate potential gradient inside the fibers, but this does not appear to present a serious problem. First it may be noted that all ultrafiltration hollow fibers are electrolytically conducting and that they are of a generally convenient size. Second the primary effect of electrical resistance in the tube wall is only to decrease the internal transverse field rather than to distort it.

The validity of this latter statement is easily demonstrated by considering an isolated fiber in semi-infinite surroundings of the same concentration as that inside the fiber (see Figure 11). For each of the three phases of this system Laplace's equation holds for the electrostatic potential ϕ. Then for our postulated two-dimensional situation

$$\nabla^2\Phi = \frac{1}{r}\frac{\partial}{\partial r}\left(r\frac{\partial\Phi}{\partial r}\right) + \frac{1}{r^2}\frac{\partial^2\Phi}{\partial\phi^2} = 0 \qquad (56)$$

and the boundary conditions are

$$\text{At} \quad r = R \quad \Phi_i = \Phi_m; \quad k\frac{\partial\Phi_i}{\partial r} = k_m\frac{\partial\Phi_m}{\partial r} \qquad (57, 58)$$

$$\text{At} \quad r = R + \delta \quad \Phi_m = \Phi_0; \quad k_m\frac{\partial\Phi_m}{\partial r} = k\frac{\partial\Phi_0}{\partial r} \qquad (59, 60)$$

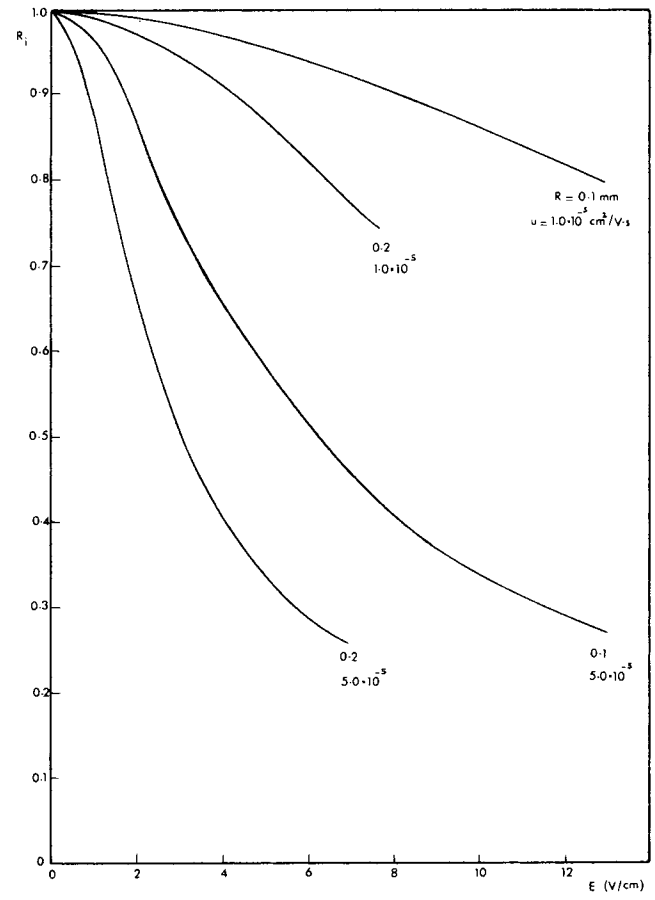

Fig. 10. Retardation factor as a function of potential gradient for representative proteins and fiber diameters.

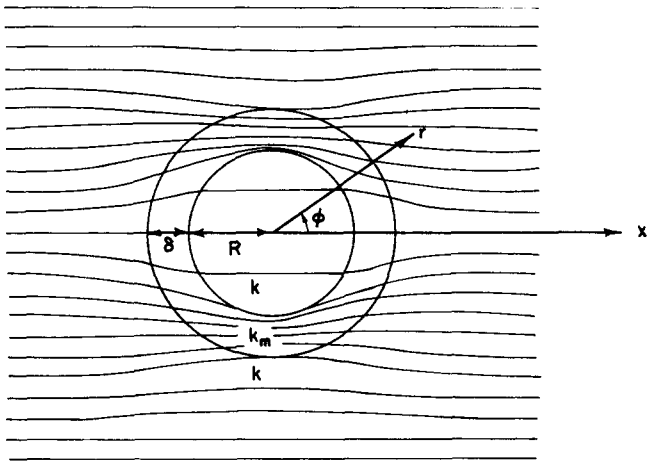

Fig. 11. Distortion of the electrical field by an isotropic fiber.

$$\text{As} \quad r \to \infty \quad \Phi_0 \to Fx = Fr\cos\phi \qquad (61)$$

Here the subscripts i, m, and 0 refer to the inside, membrane, and outside phases, respectively.

Equations (56) to (61) are satisfied by the potential profiles:

$$\Phi_0 = Fr\cos\phi + \frac{A}{r}\cos\phi$$

$$\Phi_m = Br\cos\phi + \frac{C}{r}\cos\phi$$

$$\Phi_i = Er\cos\phi$$

with

$$A = \frac{1}{2}E\left[R^2\left(1-\frac{k}{k_m}\right) + (R+\delta)^2\left(1+\frac{k}{k_m}\right)\right] - (R+\delta)^2F$$

$$B = \frac{1}{2}E\left(1+\frac{k}{k_m}\right)$$

$$C = \frac{1}{2}R^2\left(1-\frac{k}{k_m}\right)$$

$$E = 4F \Big/ \left\{\left[2+\left(\frac{k}{k_m}+\frac{k_m}{k}\right)\right] + \frac{R^2}{(R+\delta)^2}\left[2-\left(\frac{k}{k_m}+\frac{k_m}{k}\right)\right]\right\}$$

We thus find the interior field to be simply $\Phi_i = Ex$ which is of the same form as that in absence of the membrane. The situation will be more complex in a fiber bundle, but there seems no reason to expect serious practical difficulties arising in this case, so long as the fiber spacing is reasonably uniform.

ACKNOWLEDGMENTS

The authors are indebted for financial support to the National Science Foundation Grant GK33346X. In addition J. F. G. Reis wishes to acknowledge assistance provided by a Fundação Calouste Gulbenkian Fellowship.

NOTATION

c_i = concentration of species i
c_{i0} = concentration of species i in the centerline of the fiber
$\mathcal{D}_{im}$ = pseudo-binary diffusivity of species i in mixture
$\overline{D}$ = axial dispersion coefficient defined by Equation (17)
$\underline{E}$ = electrical field inside the fiber
f_k = set of functions defined by Equation (12)
k = electrical conductivity in the solution phase
k_m = electrical conductivity inside the tube wall
K = an integration constant defined in Equation (36)
L = distance traveled by solute in ultrafiltration tube during elution
M_i = total mass of solute i in tube
N_i = molar flux of species i
N_{ir} = radial component of molar flux of i
N_{iz} = axial component of molar flux of i
$Pé$ = Péclet number, $v_wR/\mathcal{D}_{im}$ or $\epsilon_iR/\mathcal{D}_{im}$
Q = any physical quantity
r = radial distance from axis of tube
R = radius of tube
R_f, R_i = retardation factor, defined in Equation (17a)
S = variable defined by Equation (45)
t = time, min.
$\overline{u}$ = average solute velocity, defined in Equation (15)
u_i = electrical mobility of species i
$\underline{v}_i$ = velocity of species i
v_r = radial component of solution's velocity
v_w = solvent velocity through the tube wall
v_z = axial component of solution's velocity
y = radial distance from the tube's wall
z = axial distance along the tube in the direction of solvent's flow

Greek Letters

δ = tube wall thickness
$\underline{\delta}_x$ = unit vector in x-direction
$\underline{\epsilon}_i$ = electrophoretic velocity, as defined by Equation (50)
ζ = dimensionless axial distance, z/L
η = dimensionless radial distance, r/R
θ = a dimensionless function of time defined by Equation (42)
λ = reciprocal of the estimated radial response time
Λ = maximum length of ultrafiltration tube, $R<v_{z0}>/2v_w$
τ = dimensionless time, v_wt/R
ϕ = polar coordinate, as in Figure 9
Φ = electrical potential

Subscripts

w = wall condition
0 = axial position at $z = 0$
∞ = large-time asymptote
$< >$ = averaging over the cross-section of the tube

LITERATURE CITED

Caldwell, K. D., L. F. Kesner, M. N. Myers, and J. C. Giddings, "Electrical Field-Flow Fractionation of Proteins," *Science*, **176**, 296 (1972).

Gill, W. N., and R. Sankarasubramanian, "Exact Analysis of Unsteady Convective Diffusion," *Proc. Roy. Soc. Lond.*, **A.316**, 341 (1970).

Kozinski, A. A., F. P. Schmidt, and E. N. Lightfoot, "Velocity Profiles in Porous-Walled Ducts," *Ind. Eng. Chem. Fundamentals*, **9**, 502 (1970).

Lightfoot, E. N., "Transport Phenomena and Living Systems," pp. 186-187, Interscience, New York (1974).

Manuscript received December 14, 1973; revision received and accepted April 8, 1974.